Studia Geotechnica et Mechanica, Vol. XXX, No. 1–2, 2008

ADVANCES IN CONSTITUTIVE MODELLING OF JOINTED ROCK HYDROMECHANICAL INTERACTIONS AT LABORATORY SCALE

PHILIPPE LOPEZ

INPL-LAEGO-ENSMN, Parc de Saurupt, Ecole des mines, 54000 Nancy, France.
Philippe.lopez@mines.inpl-nancy.fr

ALAIN THORAVAL

INERIS, Parc de Saurupt, Ecole des mines, 54000 Nancy, France.

OLIVIER BUZZI

University of Newcastle, Australia.

IRAJ RAHMANI

Transportation Research Institute, No. 19, Noor Street, Afrigha avenue, Tehran, Iran.

MARC BOULON

Laboratoire 3S (Sols, Solides, Structures), UMR 5521 (UJF, INPG, CNRS), 38041 Grenoble, France.

Abstract: This study is a part of a wide multi-scale research based on *in situ* experiments and laboratory tests. The latest, radial water injections in the centre of the lower joint wall are done at constant normal stress ranging from 0 to 110 MPa and at pressures from 0 to 4 MPa. Four hydromechanical tests have been performed in the L3S laboratory on fractured limestone samples (two diaclase and two bedding plane). The measurement analysis shows a relation between the contact surface variations and the flow values inside the fracture. The hydromechanical modelling performed using 3DEC code can be improved compared with the previous analysis due to the modification of the relation between the joint hydraulic opening and the joint mechanical closure. The gap between simulations and measurements can be related to fracture asperity degradation and turbulent flow that have not been taken into account in the modelling.

1. INTRODUCTION

When normal stress is applied to joints, the normal deformation is typically nonlinear. GOODMAN [3] and BARTON et al. [1] proposed two different hyperbolic models, widely used nowadays. EVANS et al. [2] proposed a logarithmic model to explain the nonlinear normal closure behaviour of rock joints. These three major works indi-

cate that the fracture stiffness increases as normal stress increases. Lately, LEE and HARRISON [00] used empirical parameters for non-linear fracture stiffness modelling. Furthermore, the research to link morphology with the mechanical behaviour improves, for example, in HUANG's et al. [5] work, where a mathematical model is developed for regular asperities, the deformation behaviour of a rock joint explicitly accounts for the effects of joint surface morphology. For hydraulic behaviour, a commonly used equation is the cubic law. It is derived from the fundamental principle of dynamics and is applied to a particular geometry such as a parallel plate fracture. It gives an analytical expression where the flow rate depends on the pressure gradient and the cubic fracture aperture. QIAN et al. [9] obtained the results from tests that indicate a non-Darcian turbulent flow in the fracture even though the Reynolds number is relatively low. Since the sixties of the twentieth century, the hydromechanical behaviour under normal closure has been widely studied. LONDE and SABARLY [7], using experimental results, showed a decrease in fracture transmissivity with normal stress. WITHERSPOON et al. [11] proposed a modified cubic law, introducing a factor that accounts for the roughness of the fracture surface. BARTON et al. [1] proposed an empirical model with their JRC. There has been conflicting laboratory evidence about the cubic law and the effects of contact areas. An extensive study is presented in details in the RUTQVIST's and STEPHANSSON's [10] review article. The friction factor has been introduced into a lot of different laws, with or without an exponent. A recent paper, NAZRIDOUST et al. [8], shows another empirical law in the case of laminar flow through a rock fracture. The point is that it does not represent a clear roughness measurement. In rock fractures, the Terzaghi effective stress concept is improved by considering the pressure applied to the surface contact proportion. The major objective of this work was to introduce a real measurement of the morphology in the classical laws linking the hydraulic opening with normal displacement and the normal stress with the fluid pressure.

2. LABORATORY TESTS

A series of laboratory tests and a monitoring of the evolution of the morphology have been performed on diaclase and bedding plane samples of limestone. The samples have been chosen from boreholes drilled into the limestone of the Coaraze site, close to Nice, France. The site is a medium sized superficial limestone bedrock reservoir (roughly 20 m by 20 m by 20 m) with diaclases and bedding planes. For the purpose of site experiment, quite a lot of drillings have been performed; rock and joint samples (diaclases and bedding planes) could be used for laboratory experiments. F1 and F2 are diaclase samples; JS1 and JS2 are bedding plane samples. The rock matrix is characterized by a Poisson's coefficient (ν) of 0.3, a Young's modulus and a normal strength with dispersive values: in the same direction of foliation 45 MPa < E < 62 MPa and 86 MPa

$< \sigma_c <$ 173 MPa. The tests have been carried out with the prototype developed at the laboratory 3S and called BCR3D (3D direct shear box for rock joints). It allows the hydromechanical behaviour of rock joints and the flow anisotropy to be investigated (Boulon, 1995; HANS and BOULON [4]). A general view of the device is given in figure 1.

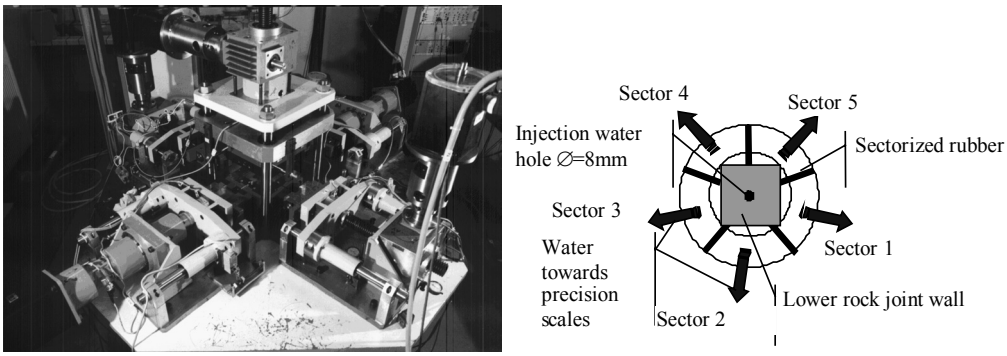

Fig. 1. General front view and hydraulic part of the BCR3D

The morphology (x, y, z) of both joint walls can be measured by a laser beam (the diameter of the beam: 0.25 mm, sampling step: 0.15 mm/128 × 128 points over a maximum surface of 110 mm per 110 mm, vertical resolution: 0.01 mm). The laser can be placed in the BCR3D to scan the surfaces so that it is not necessary to remove the sample from the shear box (figure 2). The procedure allows both joint walls to stay aligned and prevents from the matching problems at the beginning of each part of

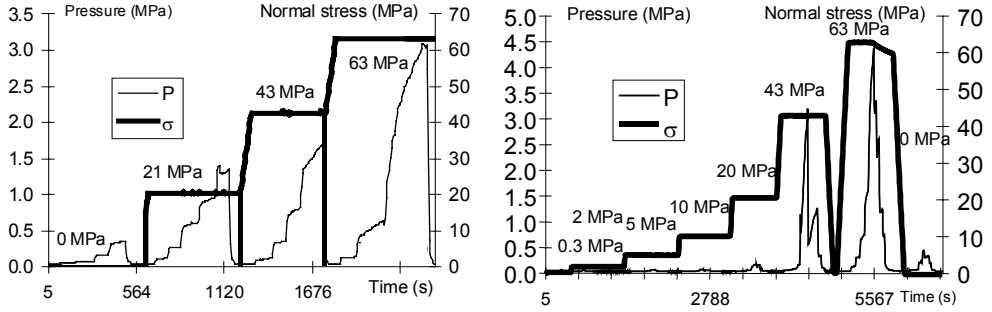

Fig. 2. The stress applied and injection hydraulic pressure for F1 (left) and JS1 (right) samples

tests. The physical values measured during a test are as follows: the normal relative displacement, the normal stress and the hydraulic parameters (the injection flow rate, the injection pressure and five outlet masses). The tests are performed according to the ISRM recommendations (Boulon, 1995). In this study, different steps of normal load are applied (loading velocity of 0.3 MPa/s) and some hydraulic excursions are

made at constant normal stress, i.e., an increase and a decrease in fluid pressure. While the stress level is constant, the water pressure rises from 0 to a maximum value, following sills; the relative normal displacement, the injection flow rate and the five output pressures are measured. For each value of the normal stress, an asymptotic value of the injection and output flow rate are reached.

For each morphology measurements two series of points (x, y, z) are known, one for the upper wall and one for the lower wall. After the upper wall has been turned upside down and the joint walls have been aligned like they are along the test, it is possible to compute the void space at each point; it is computed at a given loading stage of known normal stress and relative displacement (δ, σ_v), assuming that the deformation of an asperity does not influence the surrounding ones and that the average displacement is also the displacement for each point of the joint walls. Figure 3 shows, for F1, the evolution of σ_n against u_n and a quite constant evolution of the normal stiffness (k_n) regarding four different samples. The diaclases samples (F1 and F2) have higher normal stiffness than the bedding plane samples (JS1 and JS2) at normal stress higher than 20 MPa. At 60 MPa, an average value of diaclase normal stiffness is twice as high as the value for the bedding planes (250 GPa/m and 125 GPa/m). So the bedding planes are easier to be closed than the diaclases. This can be inferred based on the values of the classical roughness parameters, the range and the coefficient of the variation of the height.

The table shows the values for F1 and JS1. The stabilised flow rate values have been taken for each couple (σ_n; P_{inj}), see figure 4. For each value of the normal stress, an increase in the flow rate seems to be proportional to the injection pressure.

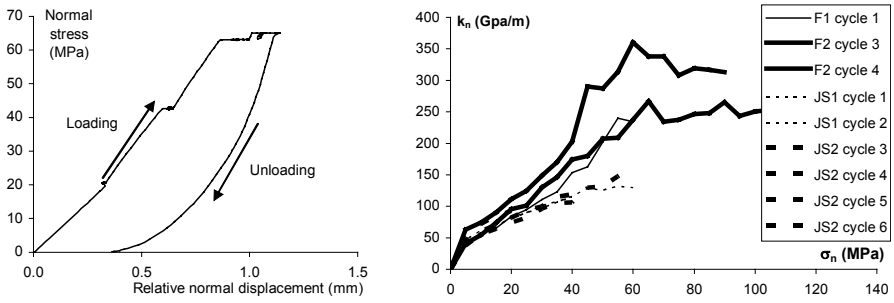

Fig. 3. σ_n against u_n for F1 sample (left) and k_n against σ_n for all samples (right)

Table

Roughness coefficients of F1 and JS1

	CLA	RMS	Range	Coef. variation
F1	3.08	3.12	3.5	0.16
JS1	4,31	4.52	8.5	0.31

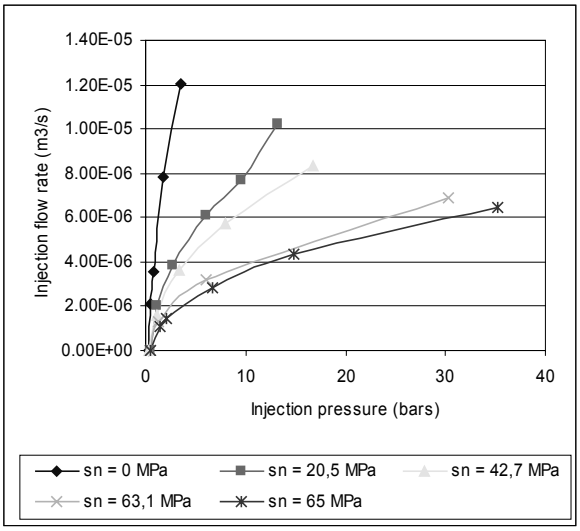

Fig. 4. Injection flow rate versus injection pressure

3. RESULTS AND DISCUSSION

3.1. HYDROMECHANICAL INTERPRETATIONS

A basic analytical interpretation of these tests, assuming the laminar and isotropic flow between two parallel joint walls, allows estimating the initial openings of the discontinuities. The intrinsic transmissivity ($T_i = K_i e$) with a radial flow takes then the following form:

$$T_i = \frac{Q\mu_w}{P2\pi} \ln\left(\frac{r_e}{r_i}\right) \tag{1}$$

with $2 \times r_e$, the external diameter; $2 \times r_i$ the internal diameter.

The values of intrinsic transmissivity, measured for the steady-state flow for each couple (σ_n; P_{inj}), are presented in figure 5.

Moreover, assuming the relation $T_i = a^3/12$ between intrinsic transmissivity and hydraulic aperture, the hydraulic opening can be computed as in the following equation:

$$a = \sqrt[3]{\frac{Q6\mu_w}{P\pi} \ln\left(\frac{r_e}{r_i}\right)}. \tag{2}$$

Figure 5 shows that the hydraulic openings decrease as the normal stress value increases. These values approach $5 \cdot 10^{-5}$ m, ranging from $1 \cdot 10^{-4}$ m to $1 \cdot 10^{-5}$ m (as the normal relative closure is related to the normal stress and the hydraulic opening). For high normal stress values, such as 90 and 110 MPa for sample F2, the hydraulic opening remains stable at the injection pressures from 0 to 4 MPa. Whereas for low normal stress it decreases from $4 \cdot 10^{-5}$ m to $3 \cdot 10^{-5}$ m. This phenomenon can be explained by an increase of the Reynolds number, as much as the flow is no longer permanent but becomes turbulent.

At very low normal stress, i.e., up to 5 MPa, figure 5 shows that the hydraulic opening rises with an increase of injection pressure. This phenomenon is observed for low injection pressure at the beginning of the injection.

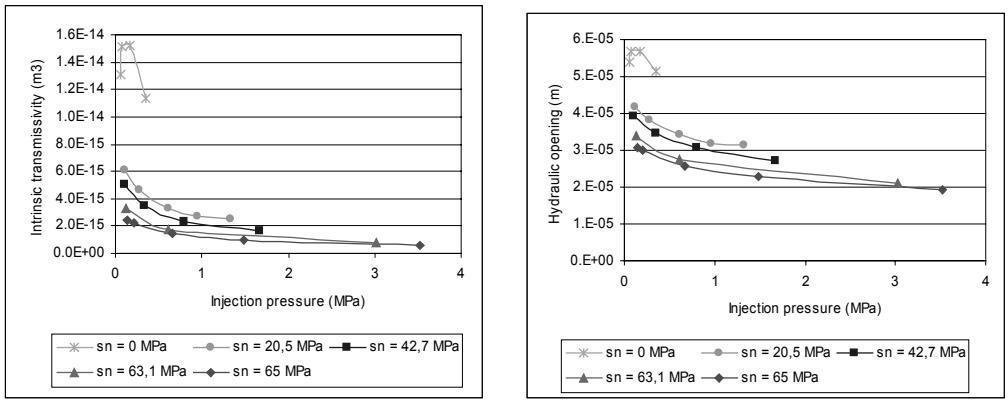

Fig. 5. Intrinsic transmissivity and hydraulic opening against injection pressure for F1

3.2. MORPHOLOGY MONITORING AND HYDROMECHANICAL INTERACTIONS

As we can calculate back the void space for each step of a test, we can study the interaction between morpho- and hydromechanical parameters. The surface is supposed to be in contact if the void space is less than 0.001 mm. For each sector, the mean value of standard deviation δ_{mean} and the coefficient of variation δ_{cv} (standard deviation divided by the average) of fracture openings are computed and compared with the outflow rate (figure 6). The relationship between the back calculated openings and the outflow rate is examined when the flow is quasi-permanent. The mean values of the openings do not follow the output flow (the same figures, δ_{mean} versus Q_{out}). Figure 6 shows that for F1 the proportion of the outflow for each sector does not depend on the normal stress level. We can assume three reasons for this difference:

- Tortuosity of the flow: it is not sectorised when the openings are sectorised; the flow is not only radial. The different channels that we could imagine in figure 6, level

63 MPa, can allow a part of the flow to be directed towards the sectors that do not have the maximum average opening, i.e., sector 1.

- From the normal stress value of 60 MPa, the hypothesis that too contiguous asperities are independent is no longer acceptable, two joint walls are damaged.
- The behaviour, e.g., elastoplastic, can no longer be ignored to calculate back the openings.

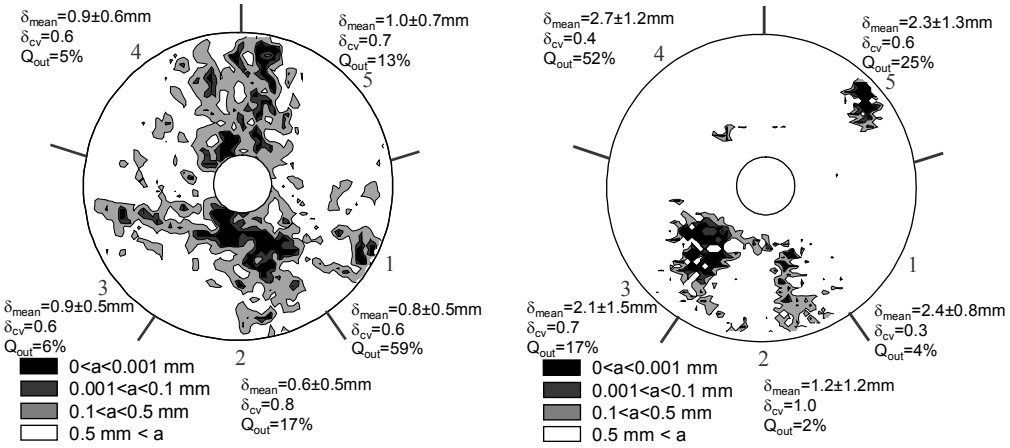

Fig. 6. F1 Morpho-hydro-mechanical scheme, 63 MPa

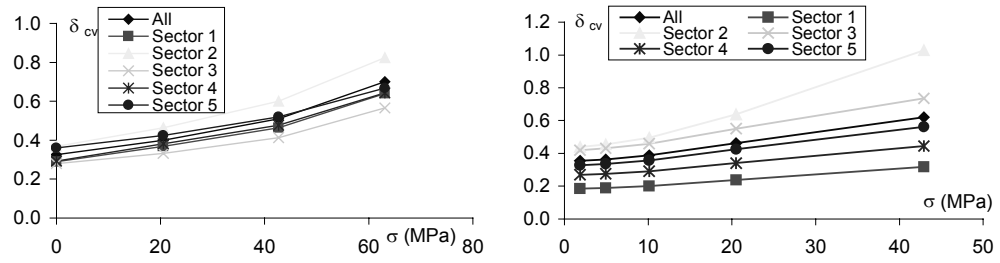

Fig. 7. F1 (left) and JS1 (right) coefficients of variation of the openings versus σ

The coefficient of variation δ_{cv} is always increasing with the normal stress (figure 7). The values of the contact surface (S_c) (figure 8) are compared with the values of the coefficient f defined by $f = \Delta a/\Delta u_n$, where a is the hydraulic opening, and u_n stands for the normal mechanical opening. For JS1 and F1 the variation of f is the same. The highest values of f are reached when the values of the contact surface increase. A turbulent flow is the main reason for the differences. The Reynolds number $Re = VD_h\rho/\mu$, where: D_h is the hydraulic diameter, ρ – the volumetric mass of water (1000 kg/m^3), μ – the dynamic viscosity (10^{-3} Pa.s), V – the flow speed (computed as a parallel flow

$Q_i/a \cdot 2 \cdot \pi \cdot r_i$, where Q_i is the injection flow rate and r_i is the injection tube diameter). Now *Re* can be expressed by:

$$Re = \frac{Q_i \cdot \rho}{\pi \cdot r_i \cdot \mu} = \frac{Q_i}{r_i} \cdot 318471 . \tag{3}$$

For F1 the flow rate ranges from $6 \cdot 10^{-6}$ to $1.2 \cdot 10^{-5}$ m^3/s, $r_i = 2.5 \cdot 10^{-3}$ m, and the Reynolds number ranges from 760 to 1520. For JS1, as the maximum flow rate approaches $2 \cdot 10^{-5}$ m^3/s, the Reynolds number maximum value is 2547. Inside the sample, the flow rate can be higher. Furthermore, the opening values are scattered. There are the zones where the values of Reynolds number are higher than the typical value of 2300. There is also a re-circulation phenomenon: it occurs when the opening increases suddenly (step phenomenon). So, there is turbulent flow in general, and locally this turbulent flow can be important.

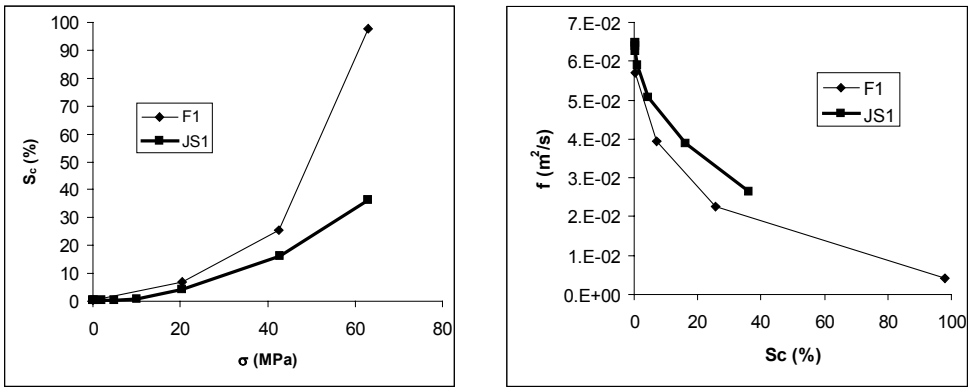

Fig. 8. S_c versus σ and f versus S_c for F1 and JS1

3.3. HYDROMECHANICAL MODELLING

To take into account the effect of a hydromechanical coupling on fracture outflow (which is not possible using the previous analytical approach), the laboratory test has been simulated using the 3DEC code. Both the fractured rock mass sample and the mortar are represented. The fracture morphology is not modelled explicitly (an equivalent fracture plane with initial constant opening is considered). This fracture, however, is discretised to allow computing the different variations of displacement, stress, pressure and flow from one grid point to another.

The following assumptions are made:

- The rock matrix and the fracture behave elastically. There is assumed coherence between the Young modulus $E = 60000$ MPa, the Poisson's ratio $\nu = 0.3$ and the labo-

ratory results. The analysis of the unloading phase of the tests shows that the fracture normal stiffness varies with the effective normal stress (k_n = 15 GPa/m for σ_n = 0 MPa; k_n = 80 GPa/m for σ_n = 20 MPa; k_n = 160 GPa/m for σ_n = 40 MPa; k_n = 240 GPa/m for σ_n = 60 MPa for F1 test).

- The flow inside the fracture follows the cubic law (applied on a mesh scale of the fracture). The initial value of the fracture hydraulic aperture has been determined previously from the analytical approach for zero (or small) effective stress ($a_0 = 6 \cdot 10^{-5}$ m for F1 test).
- The hydraulic aperture is supposed to vary during the test, depending to mechanical closing Δu_n ($\Delta a = f \cdot \Delta u_n$, where $\Delta u_n = -k_n \Delta \sigma'_n$ and f is the factor dependent on the effective normal stress σ'_n). The hydromechanical coupling is also defined by the Terzaghi–Biot relation: $\Delta \sigma'_n = \Delta \sigma_v - \beta \Delta P$. Because the hydraulic pressure variation remains small compared with stress variation during the test, this relation has been simplified by assuming $\beta = 1$.

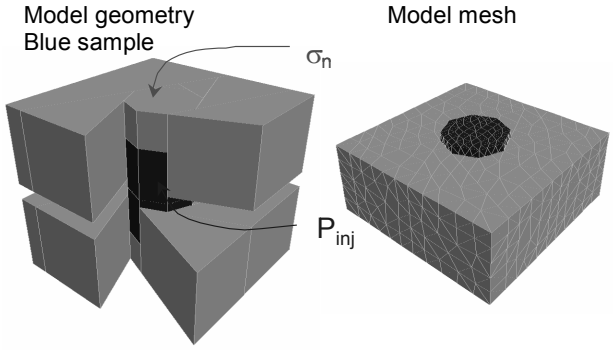

Fig. 9. 3DEC model used for test interpretation

The hydromechanical loading applied during the tests has been simplified to a series of normal stress and hydraulic pressure steps. Simulation must be regarded as a succession of steady-state calculations (one for each hydraulic pressure step). To reach balance, 3DEC carries out a certain number of hydraulic cycles, a certain number of mechanical cycles being also realized in order to obtain a mechanical balance within each hydraulic cycle. These cycles are due to the explicit character of the Distinct Element Method used. Variation between measured and calculated normal displacements, observed when the normal stress exceeds 40 MPa, can be explained by the fact that 3DEC does not simulate the irreversible normal displacements induced by the fracture wall damage. The value computed for the fracture outflow is highly dependent on the choice made for the ratio f between hydraulic aperture and mechanical closing variations. For each test, two simulations have been run: the first one as-

suming that f remains constant and is equal to 1, the second one considering the relation determined previously between f and σ_n (figure 8).

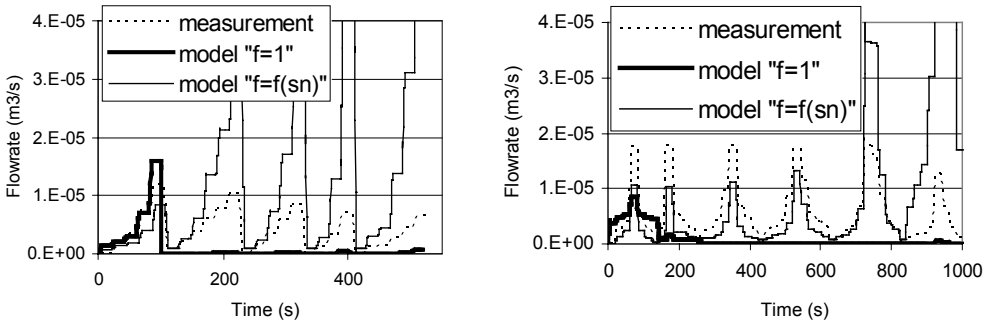

Fig. 10. Comparison between the measured and computed injection flows F1 (left) and JS1 (right)

When the experimental value f is injected in the model at low normal stress levels (up to 20 MPa), the computed flow rate values fit best with the measured flow rate values. However, the flow rate values are overestimated, especially for sample F1, for high values of normal stress and hydraulic pressure. The gap between the simulated and measured flow rates can be related to the fact that the model does not take in account the fracture asperity degradation (occurring at high normal stress) and the turbulence of the flow (occurring at high injection hydraulic pressure).

4. CONCLUSIONS

After in situ evidence for the morphological interaction with hydromechanical behaviour, hydromechanical tests with morphological monitoring are performed. The back computed void spaces allow comparing, at different normal stress, the evolution of the hydraulic opening with the normal closure. The bedding planes have a lower normal stiffness than the diaclases. The values of roughness classical parameters, the range and the coefficient of variation show that the behaviour of diaclases is stiffer than that of the bedding planes. When expressing the hydraulic opening rise (f) as a function of the contact surfaces, the bedding planes and diaclases have the same variation, but this coefficient takes higher values for JS1. Furthermore, for the normal stress lower than 20 MPa, we showed that injecting the values of the coefficient f in the model leads to a closer matching of flow rate curves. We have shown that a morphology measurement and the knowledge of the contact surface are necessary to model correctly the flow rate. However, some limitations of the numerical approach used (the turbulent flow and asperity degradation are not taken into account) do not allow the flow measurements to be closely reproduced. The morphology data meas-

ured during testing have not been used yet; we will use them to determine at what normal stress the asperity damage starts, and so to set the limit, in terms of normal stress, over which the morphology measurement at the beginning of the test cannot be carried out. We also need to analyse accurately the flow between two rough joint walls and to check whether or not a low pressure turbulence occurs.

REFERENCES

[1] BARTON N.R., BANDIS S., BAKHTAR K., *Strength, deformation and conductivity coupling of rock joints*, International Journal of Rock Mechanics and Mining Sciences & Geomechanics Abstracts, 1985, 22, 121–140.

[2] EVANS K.F., KOHL T. HOPKIRK R.J., RYBACH L., *Modelling of energy production from hot dry rock systems*, 1992, Proj Rep Eidgenössische Technische Hochschule (ETH), Zürich, Switzerland.

[3] GOODMAN, R.E., *The mechanical properties of joints*, Proc. 3rd Int. Congr. International Society of Rock Mechanics, 1–7 September, 1974, Denver, Colorado, National Academy of Sciences, Washington, DC, Vol. I, 127–140.

[4] HANS J., BOULON M., *A new device for investigating the hydro-mechanical properties of rock joints*, Int. J. Numer. Anal. Meth. Geomech., 2003, 27, 513–548.

[5] HUANG T.H., CHANG C.S., CHAO C.Y., *Experimental and mathematical modelling for fracture of rock joint with regular asperities*, Engineering Fracture Mechanics, 2002, Vol. 9, 1977–1996.

[6] LEE S.D., HARRISON J.P., *Empirical parameters for non-linear fracture stiffness from numerical experiments of fracture closure*, International Journal of Rock Mechanics and Mining Sciences, 2001, 38, 721–727.

[7] LONDE P., SABARLY F., *La distribution des perméabilités dans la fondation des barrages voûtés en fonction du champ de contrainte*, Proc. 1st Congr. Rock Mechanics, 25 Septembre–1 Octobre 1966, Lisbon, Lab. Nac. Eng. Civil., Lisbon, 1966, Vol. II, 517–522.

[8] NAZRIDOUST K., AHMADI G., SMITH D.H., *A new friction factor correlation for laminar, single-phase flows through rock fractures*, Journal of Hydrology, 2006, Vol. 329, 315–328.

[9] QIAN J., ZHAN H., ZHAO W., SUN F., *Experimental study of turbulent unconfined groundwater flow in a single fracture*, Journal of Hydrology, Vol. 311, Issues 1–4, 15 September 2005, 134–142.

[10] RUTQVIST J., STEPHANSSON O., *The role of hydromechanical coupling in fractured rock engineering*, Hydrogeology Journal, 2003, 11, Springer-Verlag, 7–40.

[11] WITHERSPOON P.A., WANG J.S.Y., IWAI K., GALE J.E., *Validity of cubic law for fluid flow in a deformable rock fracture*, Water Resour. Res., 1980, 16, 1016–1024.